INTERNATIONAL JOURNAL OF OPTIMIZATION IN CIVIL ENGINEERING
Int. J. Optim. Civil Eng., 2025; 15(3):485-510

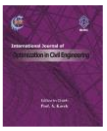

OPTIMAL DESIGN OF LARGE-SCALE DOME STRUCTURES WITH MULTIPLE FREQUENCY CONSTRAINTS USING PLASMA GENERATION OPTIMIZATION

A. Kaveh[*,†], S.M. Hosseini, and K. Biabani Hamedani
School of Civil Engineering, Iran University of Science and Technology, Tehran, Iran

[DOI: 10.22068/ijoce.2025.15.3.651]

ABSTRACT

This paper presents the application of the Plasma Generation Optimization (PGO) algorithm to the optimal design of large-scale dome trusses subjected to multiple frequency constraints. Such problems are notoriously challenging due to their highly non-linear and non-convex nature, characterized by numerous local optima. PGO is a physics-inspired metaheuristic that simulates the processes of excitation, de-excitation, and ionization in plasma generation, balancing global exploration and local refinement through its unique search mechanisms. The performance of PGO is evaluated on three well-established dome truss benchmarks: a 52-bar, a 120-bar, and a 600-bar structure, encompassing both sizing and sizing-shape optimization. A comprehensive statistical analysis based on multiple independent runs demonstrates the algorithm's effectiveness and robustness. The results show that PGO achieves the best-reported minimum weight for the 120-bar and 600-bar domes, while obtaining a highly competitive, near-optimal design for the 52-bar dome. Furthermore, PGO consistently produced low average weights across all problems, confirming its reliability. The convergence histories further validate the algorithm's efficiency in locating feasible, high-quality designs. The findings conclusively establish PGO as a powerful and reliable optimizer for handling complex structural optimization problems with dynamic constraints.

Keywords: structural optimization; frequency constraints; truss structures; metaheuristic algorithms; Plasma generation optimization.

Received: 27 August 2025; Accepted: 21 October 2025

[*]Corresponding author: School of Civil Engineering, Iran University of Science and Technology, Narmak, Tehran, P.O. Box 16846-13114, Iran
[†]E-mail address: alikaveh@iust.ac.ir (A. Kaveh)

1. INTRODUCTION

The natural frequencies of a structure are among its most critical inherent properties, as they fundamentally govern its dynamic response [1]. For systems dominated by low-frequency vibrations, the fundamental natural frequency is particularly pivotal in determining overall behavior [2]. Consequently, engineers can significantly enhance a structure's dynamic performance by strategically adjusting these frequencies. This is accomplished through optimization procedures that incorporate frequency constraints, enabling precise control over vibrational characteristics. A practical application of this is in aerospace engineering, where spacecraft design must strictly control the lowest natural frequencies to remain within specific thresholds, thereby preventing destructive resonant vibrations.

The challenge of optimizing structures subject to frequency constraints has been a fertile area of research for decades, with contributions spanning a wide range of methodological approaches. Early work in the field by Bellagamba and Yang [3] utilized nonlinear programming to achieve minimum mass in trusses, incorporating fundamental natural frequency and buckling limits among other constraints. Concurrently, Grandhi and Venkayya [2] developed an optimality criterion method rooted in uniform Lagrangian density for designs with multiple frequency constraints. The problem was further advanced by researchers like Tong and Liu [4], who created procedures for handling discrete variables under dynamic constraints, and Sedaghati et al. [5], who applied the integrated force method to optimize truss and beam systems. With the rise of metaheuristics, the strategies for tackling this problem diversified significantly. Lingyun et al. [6] introduced a Niche Hybrid Genetic Algorithm (NHGA) for combined shape and size optimization, while Gomes [7] demonstrated the effectiveness of Particle Swarm Optimization (PSO). Kaveh and Zolghadr [8] hybridized the Charged System Search (CSS) and Big Bang-Big Crunch (BB-BC) algorithms, equipping them with trap recognition for enhanced performance. Other nature-inspired methods followed, including the Orthogonal Multi-Gravitational Search Algorithm (OMGSA) by Khatibnia and Naseralavi [1] and the Cyclical Parthenogenesis Algorithm (CPA) applied by Kaveh and Zolghadr [9] to cyclically symmetric trusses. The focus on complex, large-scale structures is exemplified by the work of Kaveh and Ilchi Ghazaan [10] on dome design. More recently, algorithmic improvements have continued, with Ho-Huu et al. [11] presenting a refined Differential Evolution (DE) approach, and Lieu et al. [12] proposing a powerful hybrid between DE and the Firefly Algorithm (FA) for shape and size optimization under multiple frequency constraints.

Optimization problems involving frequency constraints are notoriously challenging due to their nonlinear and non-convex nature, often featuring a multimodal landscape of potential solutions [13]. A primary complication arises from the phenomenon of mode switching, where the sequence of a structure's natural frequencies can change as its dimensions are altered during the optimization process. This creates discontinuities that often hinder an algorithm's convergence [14]. These characteristics render classical gradient-based optimization techniques, which depend on the availability of smooth gradient information for the frequencies [6], largely ineffective for such problems. Consequently, metaheuristic algorithms, which are derivative-free, present themselves as a robust alternative for navigating this complex search space.

Metaheuristic optimization algorithms have emerged as a prominent class of approximate

[DOI: 10.22068/ijoce.2025.15.3.651]

solution methods, garnering significant research interest within computer science and engineering in recent years [15-18]. Their principal strength lies in effectively locating high-quality, near-optimal solutions for computationally complex challenges, including those classified as NP-hard, within a practical timeframe [19]. The widespread adoption of metaheuristics across various engineering disciplines is largely attributed to their key benefits: they are generally straightforward to conceptualize and code, they operate without requiring derivative information, and their flexibility makes them suitable for a broad spectrum of problem types.

The field of metaheuristic optimization has witnessed rapid advancement in recent decades, with numerous algorithms emerging from diverse sources of inspiration. Foundational methods that have shaped the discipline include the Genetic Algorithm (GA) by Holland [20], Simulated Annealing (SA) by Kirkpatrick et al. [21], and Particle Swarm Optimization (PSO) by Kennedy and Eberhart [22]. Subsequent significant contributions encompass Ant Colony Optimization (ACO) [23], Artificial Bee Colony (ABC) [24], Differential Evolution (DE) [25], and the Cuckoo Search (CS) algorithm [26]. More recent developments include the Teaching-Learning-based Optimization (TLBO) [27], Bat Algorithm (BA) [28], and Grey Wolf Optimizer (GWO) [29]. Parallel to these developments, the first author and his research team have contributed several physics-inspired metaheuristics to this growing body of literature. These include the Charged System Search (CSS) [30], Ray Optimization (RO) [31], Dolphin Echolocation (DE) [32], Colliding Bodies Optimization (CBO) [33], Water Evaporation Optimization (WEO) [34], Thermal Exchange Optimization (TEO) [35], Doppler Effect-Mean Euclidian Distance Threshold (DE-MEDT) optimization algorithm [36], among others.

Plasma Generation Optimization (PGO) algorithm is a newly developed population-based metaheuristic proposed by Kaveh et al [37]. The basic rules of the PGO are inspired by the process of plasma generation. Simulating the process of the excitation, de-excitation, and ionization that lead to plasma generation are performed based on the specific mechanisms presented in quantum physics. In the proposed method, electrons are considered as the agents of the algorithm. Moving the electrons and changing their energy levels in the search space are controlled by the algorithm parameters. Changing the position of the electrons is such that the accumulation of them occur from lower to higher energy level and in parallel with increasing gas ions in the plasma. Motivated by efficiency and appropriate penitential of the PGO algorithm, this study aims to employ this optimizer for solving truss optimization with natiral frequncy constraints.

Building upon the successful applications of PGO in civil engineering, including optimization-based damage detection [38], skeletal structure design [39], and retaining wall optimization [40], this algorithm has consistently demonstrated high performance across various complex problems. Motivated by these proven capabilities, this paper investigates the application of the standard PGO algorithm to frequency-constrained truss optimization. The algorithm is particularly suitable for such challenges due to its physically inspired search mechanism: the ionization process, which utilizes a Lévy flight distribution, enhances global exploration, while the excitation and de-excitation processes enable refined local search. To evaluate its efficacy, three dome-like truss optimization problems with multiple frequency constraints are examined, encompassing both size and shape variables. The results are rigorously compared with those from other state-of-the-art metaheuristics. Findings indicate

[DOI: 10.22068/ijoce.2025.15.3.651]

that the PGO approach is highly competitive, frequently yielding lighter feasible designs and exhibiting a robust convergence rate.

The rest of this paper is organized as follows: The standard PGO algorithm is reviewed in Section 2. In Section 3, the formulation of the truss optimization problem with natural frequency constraints is detailed. Three numerical examples are studied in Section 4. Finally, some concluding remarks are provided in Section 5.

2. PLASMA GENERATION OPTIMIZATION

The Plasma Generation Optimization (PGO) algorithm is a recently-developed metaheuristic, proposed by Kaveh et al. [37], which draws its inspiration from the physical phenomena observed in plasma generation. This algorithm conceptualizes candidate solutions as electrons, whose fitness or quality is analogous to their energy level. The core of PGO's search mechanism involves the iterative update of these electron positions by emulating three key physical processes: excitation, de-excitation, and ionization. These processes are applied repetitively to guide the population toward the optimal region of the search space. A schematic representation of these mechanisms is provided in Fig. 1, which illustrates that excitation and de-excitation govern the transitions of bound atomic electrons, whereas ionization involves liberating electrons into the plasma. To simulate the movement of these free electrons, the algorithm employs a Lévy distribution. The heavy-tailed characteristic of this distribution enables occasional long-distance steps, thereby significantly enhancing the diversity of the search trajectories. As is standard for population-based algorithms, PGO begins by initializing a population of electrons randomly within the search boundaries, as defined by the following equation:

$$e_{i.j}^{0} = e_{j.min} + rand \times \left(e_{j.max} - e_{j.min}\right) \; ; \; i = 1.2. \ldots . nE \; and \; j = 1.2. \ldots . nV \qquad (1)$$

Here, $e_{i,j}^{0}$ denotes the starting position of the j-th design variable for the i-th electron. The parameters $e_{j,\min}$ and $e_{j,\max}$ define the permissible lower and upper bounds for the j-th variable, respectively. A random number generator, rand, produces values uniformly between 0 and 1 to ensure a stochastic initialization. The total population size is governed by nE (number of electrons), while nV represents the number of design variables in the optimization problem.

During the main iterative procedure of PGO, every electron e_i in the population is compared against another electron e_{rs}, chosen at random. The algorithm evaluates their performance based on their penalized cost function values, $PCost$. If electron e_i possesses a superior solution (i.e., $\mathrm{PCost}_i < \mathrm{PCost}_{rs}$), it is attracted towards the position of e_{rs}. Conversely, if e_i is inferior, it is repelled away from e_{rs} to explore other regions. This fundamental comparative logic is mathematically expressed as follows:

$$\Delta x_i = \begin{cases} e_i - e_{rs} & PCost_i < PCost_{rs} \\ e_{rs} - e_i & PCost_i \geq PCost_{rc} \end{cases} \qquad (2)$$

[DOI: 10.22068/ijoce.2025.15.3.651]

Here, e_i and e_{rs} represent the position vectors of the two compared electrons, each comprising nV design variables. The terms PCost_i and PCost_{rs} denote the corresponding penalized objective function values for the i-th electron and the randomly selected electron, respectively.

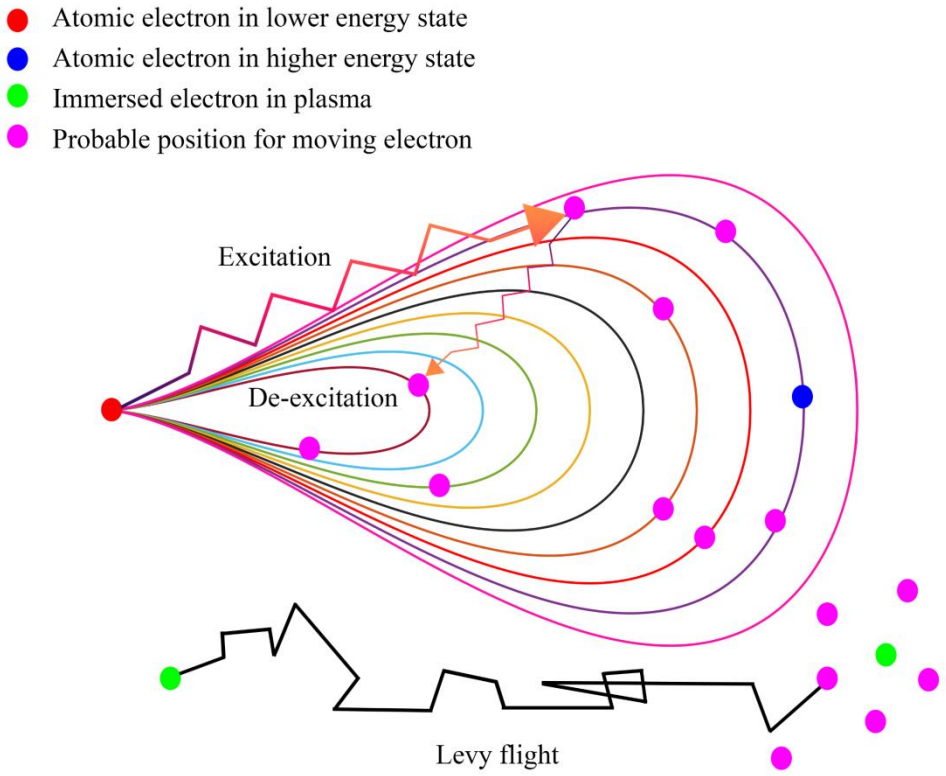

Figure 1: Simulation of excitation, de-excitation, and ionization processes occurring through the plasma generation

The subsequent phase of the algorithm executes the physical processes that simulate plasma generation: excitation, de-excitation, and ionization. Each process is governed by a unique step size calculation. The process selection begins by generating a uniform random number, rand_1, in the range [0, 1]. This value determines the primary search operation for electron e_i. If rand_1 is less than a predefined parameter called the Excitation De-excitation Rate (EDR), the excitation process is executed. Conversely, if $\text{rand}_1 \geq$ EDR, the ionization process is performed.

Furthermore, when the excitation process is activated, a secondary random number rand_2 is generated. A de-excitation process may subsequently occur if rand_2 is less than another control parameter, the De-excitation Rate (DR). The following condition summarizes the process selection logic.

[DOI: 10.22068/ijoce.2025.15.3.651]

$$\begin{cases} if rand_1 < EDR & Excitation\ \ process\ occurs \\ if\ rand_1 < EDR\ and\ rand_2 < DR & De-excitation\ process\ occurs \\ if rand_1 \geq EDR & Inoinization\ process\ occurs \end{cases} \quad (3)$$

2.1 Excitation process

During the excitation phase, electrons representing lower-quality solutions (lower energy levels) are driven toward those with higher-quality solutions (higher energy levels). To computationally emulate this transition, the electron's movement is decomposed into two orthogonal components: longitudinal transfer (LT) and transverse transfer (TT).

$$stepsize_{i.j}^{Excitation} = \overbrace{randa \times \Delta x_{i.j}}^{LT_{i.j}} + \overbrace{randb \times \Delta x_{i.j} \times (1-t)}^{TT_{i.j}} \qquad t = \frac{it}{Maxit} \quad (4)$$

in which $randa$ and $randb$ are random numbers uniformly distributed in $[0.6 + 0.1 \times \mathrm{t}, 1.4 - 0.1 \times t]$ and $[-\delta y_{i,j}, \delta y_{i,j}]$ intervals, respectively. it and $Maxit$ are, respectively, the current iteration and the maximum number of iterations as stopping criterion of the PGO. $\delta y_{i,j}$ is the transverse characteristic, obtained as follows:

Here, $randa$ and $randb$ represent adaptive random parameters. The value of $randa$ is sampled from a uniformly distributed range $[0.6 + 0.1 \times \mathrm{t}, 1.4 - 0.1 \times t]$, while $randb$ is drawn from a symmetric interval $[-\delta y_{i,j}, \delta y_{i,j}]$. The variable t denotes a progress parameter, calculated as the ratio of the current iteration number it to the maximum allowed iterations $Maxit$. The transverse characteristic $\delta y_{i,j}$ controls the exploration magnitude perpendicular to the main search direction and is determined by the following expression:

$$\delta y_{i,j} = \sqrt{\frac{\left| randa \times \left(\frac{|e_{i,j} - e_{rs,j}|}{e_{j,max} - e_{j,min}} \right)^3 - \left(\frac{|e_{i,j} - e_{rs,j}|}{e_{j,max} - e_{j,min}} \right)^4 \right|}{2 \times it}} \quad (5)$$

In this formulation, $e_{i.j}$ and $e_{rs.j}$ designate the locations of the j-th design variable for the i-th electron and the randomly selected electron, respectively. The parameters $e_{j.\max}$ and $e_{j.\min}$ define the upper and lower bounds of the allowable range for the j-th design variable.

2.2 De-excitation process

As specified by Equation (3), the de-excitation process is activated when both conditions $\mathrm{rand}_1 < \mathrm{EDR}$ and $\mathrm{rand}_2 < \mathrm{DR}$ are satisfied. This phase simulates the physical phenomenon where excited electrons lose energy by emitting photons, causing them to transition from higher to lower energy states. Within the algorithm, this is computationally represented by introducing stochastic perturbations to the positions of selected electrons, effectively redirecting them toward regions of the search space associated with lower energy levels.

[DOI: 10.22068/ijoce.2025.15.3.651]

$$stepsize_{i,k}^{De-excitation} = stepsize_{i,k}^{Excitation} + randn \times \left(e_{k,max} - e_{k,min}\right) \quad (6)$$

where

$$k = randsample(nV, NDRS) \;\; ; \;\; NDRS = ceil(DRS \times nV) \quad (7)$$

Here, the parameter DRS (De-excitation Rate for excited-state electrons) determines the proportion of design variables that undergo modification during the de-excitation phase. The number of affected dimensions, NDRS, is calculated as the smallest integer greater than or equal to the product of DRS and the total number of design variables (nV). The specific design variables to be modified are identified by the index set k, which contains NDRS distinct integers randomly selected from the range 1 to nV. The perturbation magnitude is scaled by $randn$, a random value drawn from a standard normal distribution with zero mean and unit variance.

2.3 Ionization process

The ionization process models the behavior of electrons liberated from atomic bonds and immersed in plasma, with their trajectories following a Lévy distribution. This movement pattern is mathematically represented by the step size calculation:

$$stepsize_{i,j}^{Ionization} = randn \times S_{i,j} \times \Delta x_{i,j} \times (1 - t) \quad (8)$$

where randn denotes a random variable from a standard normal distribution (mean = 0, variance = 1). The terms $\Delta x_{i,j}$ and t are derived from Equations (2) and (4), respectively. The scaling factor $S_{i,j}$ is computed as:

$$S_{i,j} = \frac{randn_1}{|randn_2|^{\frac{1}{\beta}}} \times \sigma \quad (9)$$

Here, β is a constant parameter set to 1.5, while randn_1 and randn_2 are independent normally distributed random numbers. The parameter σ is defined by:

$$\sigma = \left(\frac{\Gamma(1+\beta) \times sin\left(\frac{\pi\beta}{2}\right)}{\Gamma\left(\frac{1+\beta}{2}\right) \times \beta \times 2^{\left(\frac{\beta-1}{2}\right)}} \right)^{\frac{1}{\beta}} \;\; ; \;\; \Gamma(x) = (x-1)! \quad (10)$$

The incorporation of Lévy flight in the ionization phase significantly enhances the algorithm's diversification capability by enabling occasional long-range exploration jumps within the search space.

The new position of the *j*-th design variable of the *i*-th electron is determined as follows:

[DOI: 10.22068/ijoce.2025.15.3.651]

$$e_{i.j}^{iteration+1} = e_{i.j}^{iteration} + \begin{cases} stepsize_{i.j}^{Excitation} & Excitation\ \ process\ occurs \\ stepsize_{i.k}^{De-excitation} & De-excitation\ process\ occurs \\ stepsize_{i.j}^{Ionization} & Ionization\ process\ occurs \end{cases} \quad (11)$$

Following position updates, each newly generated electron is evaluated against its predecessor. The solution with the superior fitness (lower objective function value) is retained. Additionally, the best solution found in the current iteration is compared with the global best solution encountered thus far, with the better solution preserved as the new global best.

This iterative procedure continues until the predetermined maximum number of iterations ($Maxit$) is reached. The flowchart of the PGO algorithm is illustrated in Figure 2.

3. FORMULATION OF TRUSS OPTIMIZATION WITH FREQENCY CONSTRAINTS

This study applies the Plasma Generation Optimization (PGO) algorithm to solve size and shape optimization problems for truss structures subject to frequency constraints. The optimization aims to identify the design configuration that yields the minimum structural weight while ensuring that specified natural frequency limits are satisfied. The mathematical formulation of this constrained optimization problem is expressed as follows [13, 41]:

$$\text{Find } \{X\} = [x_1 . x_2 . \dots . x_{nDV}] \quad (12)$$

$$\text{to minimize } P(\{X\}) = f(\{X\}) \times f_{penalty}(\{X\}) \quad (13)$$

$$\text{subject to: } \begin{cases} \omega_j \geq \omega_j^* & \text{for some natural frequencies } j \\ \omega_k \leq \omega_k^* & \text{for some natural frequencies } k \\ x_i^L \leq x_i \leq x_i^U & i = 1.2. \dots . nDV \end{cases} \quad (14)$$

The vector $\{X\}$ contains the design variables for the optimization problem, where nDV represents the total number of these variables and x_i refers to the i-th design variable. The primary goal of this weight minimization problem is to reduce the objective function $f(\{X\})$, which corresponds to the total weight of the truss structure. To manage the problem constraints, a penalty function $f_{penalty}(\{X\})$ is incorporated, leading to the combined penalized objective function $P(\{X\})$ that is ultimately minimized. Each design variable x_i is constrained within a specified range, defined by its lower bound x_i^L and upper bound x_i^U.The optimization must also satisfy frequency constraints, where ω_j and ω_k represent the j-th and k-th natural frequencies of the structure, with ω_j^* and ω_k^* denoting their respective lower and upper allowable limits.

[DOI: 10.22068/ijoce.2025.15.3.651]

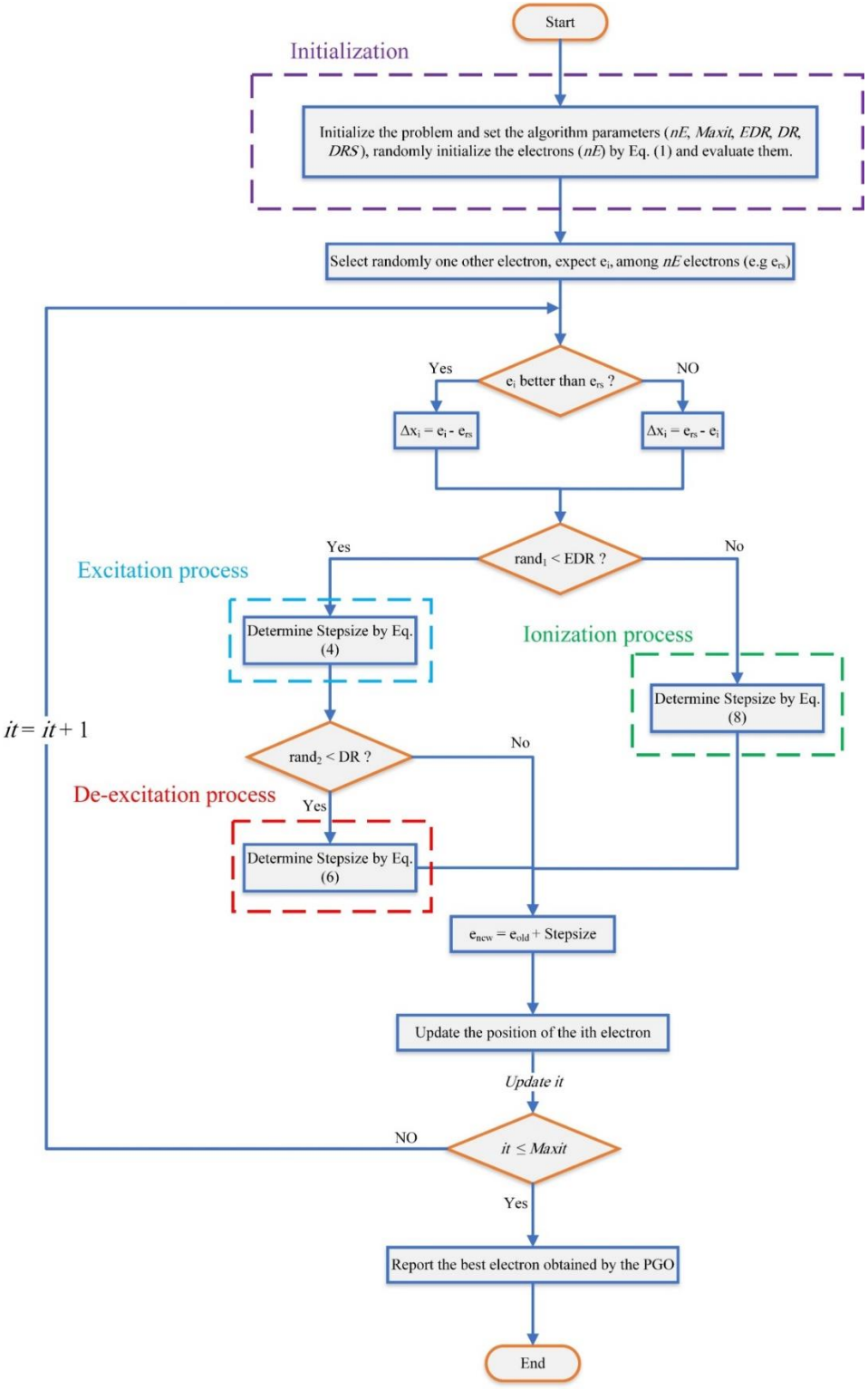

Figure 2: Flowchart of the PGO algorithm

[DOI: 10.22068/ijoce.2025.15.3.651]

The objective function, representing the total weight of the truss structure, is calculated using the following expression:

$$W(\{X\}) = \sum_{i=1}^{nE} \rho_i \times A_i \times L_i \tag{15}$$

where $W(\{X\})$ represent the weight of the truss structure; nE is the number of structural members; ρ_i is the material density; A_i is the cross-sectional area; and L_i is the length of the i-th structural member.

Penalty functions are used in order to transform a constrained optimization problem into an unconstrained one. Here, a dynamic penalty function is employed as follows [8, 42]:

$$f_{penalty}(X) = (1 + \varepsilon_1 \times \upsilon)^{\varepsilon_2};\ \upsilon = \sum_{i=1}^{nC} \upsilon_i \tag{16}$$

where nC is the number of frequency constraints; υ denotes the sum of the violations of the problem constraints; and ε_1 and ε_2 are parameters that determine the behavior of penalty function. The values of υ_i $(i = 1.2. \ldots . nC)$ are set to zero for satisfied constraints, while in case of violated constraints, they are selected considering the severity of violation. This can be expressed as follows:

$$\upsilon_i = \begin{cases} \left|1 - \dfrac{\omega_i}{\omega_i^*}\right| & \text{if the } i-\text{th frequency constraint is violated} \\ 0 & \text{otherwise} \end{cases} \tag{17}$$

The calibration of parameters ε_1 and ε_2 is crucial as they govern the penalty's severity applied to constraint violations, thereby directly influencing the algorithm's balance between exploratory search (diversification) and refined local search (intensification) [43]. An effective strategy employs a dynamically adjusted penalty where violations are treated leniently during initial iterations, permitting extensive exploration of the search space, including infeasible regions. As the optimization progresses, the penalty severity is systematically increased, gradually shifting focus toward the exploitation of promising feasible regions [9]. This dynamic adjustment promotes a balanced search process. In the present study, this is achieved by maintaining ε_1 at a constant value of 1.0, while ε_2 is linearly increased from an initial value of 1.5 to a final value of 6 over the course of the iterations.

The natural frequencies (ω_n) and corresponding mode shapes (ϕ_n) required for evaluating the constraints are determined by solving the generalized eigenvalue problem for an undamped structural system [44]:

$$k\phi_n = \omega_n^2 m\phi_n \tag{18}$$

where k and m denote the stiffness and mass matrices of the system, respectively; ω_n

[DOI: 10.22068/ijoce.2025.15.3.651]

is the n-th natural frequency of vibration of the system ($1 = 1.2.\ldots.N$); and ϕ_n is the n-th natural mode of vibration of the system. N is the number of degrees of freedom of the system.

4. CASE STUDIES

This section evaluates the performance of the Plasma Generation Optimization (PGO) algorithm by applying it to three well-established dome truss optimization problems with frequency constraints. The selected examples include a 52-bar dome (small-scale), a 120-bar dome (mid-scale), and a 600-bar dome (large-scale), serving to demonstrate the algorithm's scalability and robustness. The material properties, design variable boundaries, and frequency constraints for all three structures are summarized in Table 1.

To facilitate a rigorous statistical comparison, the results from 20 independent runs for each problem are reported, including the best weight, worst weight, average weight, and standard deviation. The computational effort is measured by the maximum number of finite element analyses (MaxNFEs). Based on recommendations from foundational PGO studies [37-40], a population size of 30 individuals was selected for all numerical examples in this investigation. This parameter configuration was found to provide an effective balance between computational efficiency and thorough search space exploration, consistently yielding superior performance across various structural optimization problems. Consequently, the population size (NP) was set to 30 for all examples. The MaxNFEs was established at 20,000 for the 52-bar and 120-bar domes, and 30,000 for the more computationally demanding 600-bar dome. For direct comparison with other algorithms reported in the literature, the optimal design from the best run is presented in detail. The PGO algorithm and the accompanying finite element analysis code were implemented in the MATLAB programming environment. The internal parameters of the PGO algorithm, which govern its search dynamics, were calibrated for the execution of these numerical studies. The selected values are as follows [37-40]: EDR=0.6, DR=0.3, and DRS=0.15. These parameters collectively control the transition probabilities between the algorithm's core physical processes, thereby balancing its exploratory and exploitative behavior.

Table 1: Material properties, cross-sectional area bounds, and frequency constraints of various problems

Problem	Elasticity modulus E ($\mathrm{N/m^2}$)	Material density ρ ($\mathrm{kg/m^3}$)	Material density ρ ($\mathrm{kg/m^3}$)	Frequency constraints (Hz)
52-bar dome-like truss	2.1×10^{11}	7800	$0{,}0001 \le A_i \le 0{,}01$	$\omega_1 \le 50/\pi, \omega_2 \ge 90/\pi$
120-bar dome-like truss	2.1×10^{11}	7971.81	$0{,}0001 \le A_i \le 0{,}01$	$\omega_1 \ge 9, \omega_2 \ge 11$
600-bar dome-like truss	2.1×10^{11}	7850	$0{,}0001 \le A_i \le 0{,}01$	$\omega_1 \ge 5, \omega_3 \ge 7$

4.1 A 52-bar dome-like truss

The first benchmark problem involves a combined sizing and geometry optimization of a

[DOI: 10.22068/ijoce.2025.15.3.651]

52-bar dome truss, where both cross-sectional areas and nodal coordinates serve as design variables. The initial structural configuration is shown in Figure 3. Under symmetrical constraints, all unconstrained nodes are permitted to shift up to ±2 m from their original positions. This results in a total of 13 design variables: eight correspond to member cross-sectional areas, and five control the nodal coordinates. Table 2 outlines the grouping of structural members based on symmetry. Material properties, frequency constraints, and bounds on cross-sectional areas are provided in Table 1. Additionally, a non-structural mass of 50 kg is applied to each free node. To ensure statistical reliability, twenty independent optimization runs were conducted. The best-performing result from these runs is reported herein to facilitate a consistent comparison with results from other optimization algorithms documented in the literature. This problem has been studied by several researchers by using various optimization methods: Miguel and Miguel [45] using Harmony Search (HS) and Firefly Algorithm (FA), Kaveh and Zolghadr [46] utilizing a hybridized CSS-BBBC algorithm, Kaveh and Zolghadr [47] employing Democratic Particle Swarm Optimization (DPSO), Ho-Huu et al. [48] by using Improved Differential Evolution (IDE), and Kaveh and Ilchi Ghazaan utilizing [49] hybridized optimization algorithms.

A comparative assessment of the optimal designs for the 52-bar dome-like truss, as presented in Table 2, demonstrates the competitive performance of the PGO method. The PGO algorithm achieves the lightest recorded best weight of 193.1936 kg, slightly outperforming other methods such as DE and IDE. Furthermore, the average weight and worst weight solutions found by PGO are highly competitive, indicating its consistent performance across multiple runs. While the standard deviation associated with PGO is higher than that of some other algorithms, its ability to consistently find very low-weight designs underscores its effectiveness.

In terms of computational expense, PGO converges to its optimal design using 18,660 finite element (FE) analyses. This represents a lower computational demand compared to the DE method, which required 20,002 analyses, though it is slightly higher than the IDE's requirement of 12,191 analyses. This balance between solution quality and computational effort highlights the efficiency of the PGO approach.

The first five natural frequencies of the optimal design found by PGO are listed in Table 3. The data confirms that all frequencies for the PGO design satisfy the imposed constraints. Similar to the trends observed with other methods, the second natural frequency appears to be the governing constraint for this structural design problem.

Finally, an examination of the convergence history, illustrated in Figure 4, reveals the characteristic search trajectory of the PGO algorithm. The plot shows a steady and pronounced decline in both the best and average penalized weights, demonstrating the method's effective and stable convergence towards the optimal design region. This further corroborates the robustness of the PGO algorithm in solving this structural optimization problem.

[DOI: 10.22068/ijoce.2025.15.3.651]

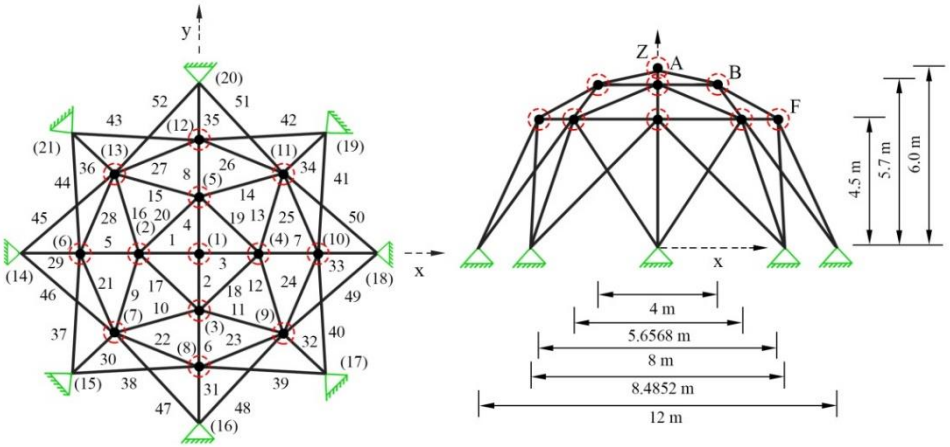

Figure 3: Initial layout of the 52-bar dome-like truss: (a) top view, (b) side view

Table 2: Comparison of optimal results of the 52-bar dome-like truss obtained by different algorithms

Design variable Z_i, X_i (m); A_j (cm^2)	HS [45]	FA [45]	CSS-BBBC [46]	DPSO [47]	DE [47]	IDE [47]	ALC-PSO [49]	PGO
Z_A	4.7374	6.4332	5.331	6.1123	6.0136	6.0052	5.6972	5.9280
X_B	1.5643	2.2208	2.134	2.2343	2.2802	2.3004	2.0008	2.2209
Z_B	3.7413	3.9202	3.719	3.8321	3.7488	3.7332	3.7000	3.7282
X_F	3.4882	4.0296	3.935	4.0316	3.9980	4.0000	3.8052	3.9508
Z_F	2.6274	2.5200	2.500	2.5036	2.5000	2.5000	2.5000	2.5000
$A_{1\text{-}4}$	1.0085	1.0050	1.0000	1.0001	1.0000	1.0001	1.0000	1.0000
$A_{5\text{-}8}$	1.4999	1.3823	1.3056	1.1397	1.0981	1.0875	1.395	1.1571
$A_{9\text{-}16}$	1.3948	1.2295	1.4230	1.2263	1.2132	1.2135	1.3184	1.2354
$A_{17\text{-}20}$	1.3462	1.2662	1.3851	1.3335	1.4227	1.4460	1.5027	1.4424
$A_{21\text{-}28}$	1.6776	1.4478	1.4226	1.4161	1.4217	1.4315	1.3888	1.3996
$A_{29\text{-}36}$	1.3704	1.0000	1.0000	1.0001	1.0001	1.0000	1.0000	1.0000
$A_{37\text{-}44}$	1.4137	1.5728	1.5562	1.5750	1.5770	1.5623	1.724	1.5864
$A_{45\text{-}52}$	1.9378	1.4153	1.4485	1.4357	1.3722	1.3724	1.3187	1.3741
Best weight (kg)	214.94	197.53	197.309	195.351	193.2481	193.2085	196.27	193.1936
Average weight (kg)	229.88	212.80	-	198.71	196.0585	196.0478	207.13	198.5633
Worst weight (kg)	-	-	-	-	202.4296	202.4215	-	231.1741
Standard deviation (kg)	12.44	8.44	-	13.85	4.1708	4.1823	6.36	12.5918
Number of FE analyses	20000	1000	4000	6000	20002	12191	9000	18,660

[DOI: 10.22068/ijoce.2025.15.3.651]

Table 3: Natural frequencies (Hz) of the optimal designs for the 52-bar dome-like truss

Frequency number	HS [45]	FA [45]	CSS-BBBC [46]	DPSO [47]	DE [47]	IDE [47]	ALC-PSO [49]	PGO
1	12.2222	11.3119	12.987	11.315	11.5319	11.6033	10.4619	11.3146
2	28.6577	28.6529	28.648	28.648	28.6494	28.6481	28.6479	28.6479
3	28.6577	28.6529	28.679	28.648	28.6509	28.6481	28.6480	28.6479
4	28.6618	28.8030	28.713	28.650	28.6509	28.6490	28.7129	28.6484
5	30.0997	28.8030	30.262	28.688	28.6661	28.6530	28.8922	28.7052

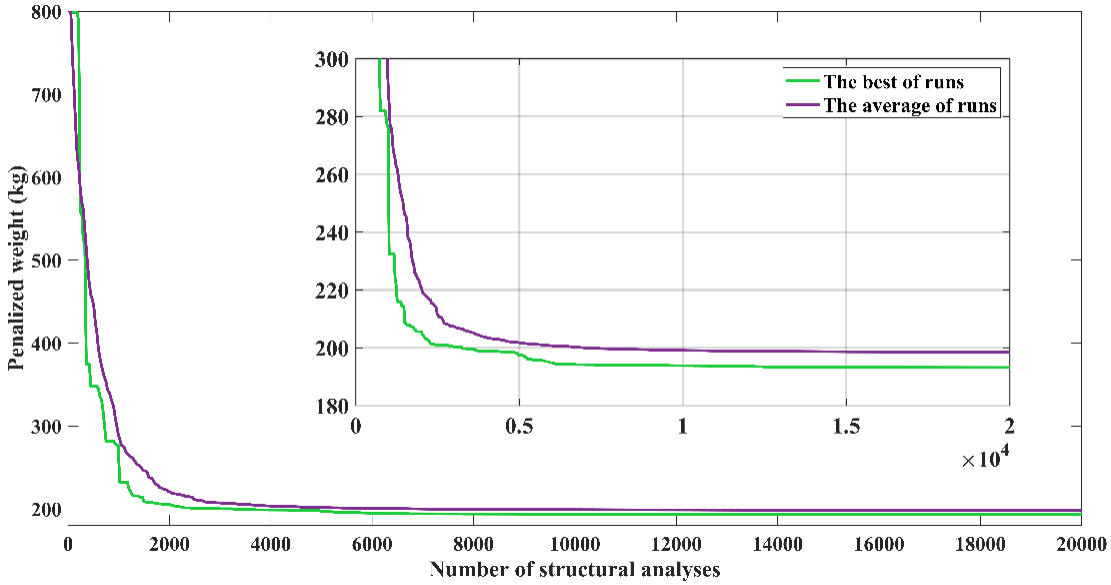

Figure 4: The best and average weight convergence histories for the 52-bar dome-like truss

4.2 A 120-bar dome-like truss

The second numerical example involves the size optimization of a 120-bar dome truss, the layout of which is presented in Figure 5. The geometry of the structure remains fixed during the optimization process. Owing to structural symmetry, the members are categorized into seven distinct groups, resulting in a total of seven sizing design variables. The material properties, constraints on natural frequencies, and permissible bounds for the cross-sectional areas are consistent with the previous example and are summarized in Table 1. Non-structural masses are applied to the free nodes to simulate additional operational weight. A mass of 3000 kg is located at the central node (node 1), 500 kg at the intermediate ring nodes (nodes 2 through 13), and 100 kg at the remaining outer nodes. To ensure statistical reliability, twenty independent optimization runs were performed. The design corresponding to the best-performing run is reported in the subsequent section for comparison with established results from the literature. This problem has been solved with various methods by different researchers: Khatibinia and Naseralavi [1] using Orthogonal Multi-Gravitational Search Algorithm (OMGSA), Tejani et al. [50] employing Improved Symbiotic Organisms Search (ISOS), Kaveh and Zolghadr [47] by using Democratic Particle Swarm Optimization (DPSO),

[DOI: 10.22068/ijoce.2025.15.3.651]

Kaveh and Zolghadr [51] utilizing Particle Swarm Ray Optimization (PSRO), Taheri and Jalili [52] using Enhanced Biogeography-Based Optimization (EBBO), Dede et al. [53] using Jaya algorithm, and Tejani et al. [54] using a Modified Sub-Population Teaching-Learning-based Optimization (MS-TLBO).

A comparative evaluation of the optimal designs for the 120-bar dome-like truss, as detailed in Table 4, highlights the superior performance of the PGO algorithm. The results indicate that PGO achieves the most lightweight structure among all compared methods, with a best weight of 8707.34 kg. Furthermore, PGO demonstrates exceptional consistency, yielding the best average weight and a highly competitive worst weight. The low standard deviation value further confirms the robustness and reliability of the PGO approach in repeatedly locating high-quality solutions across multiple runs.

In terms of computational demand, PGO required 18,780 finite element analyses to converge to the optimal design. While this is a higher number of analyses compared to several other algorithms, the superior quality and consistency of the final results justify the computational investment, establishing a favorable trade-off between performance and resource expenditure.

The natural frequencies for the PGO-optimized design, presented in Table 5, confirm that all constraints are successfully met. The data shows that the first frequency is the active constraint for this structural problem, as its value is precisely at the specified lower limit of 9.0000 Hz.

The convergence history, illustrated in Figure 6, provides insight into the search efficiency of the PGO algorithm. The plot shows a rapid and steady decline in structural weight, demonstrating the method's effective and direct trajectory toward the global optimum region. This efficient convergence behavior further solidifies the capability of PGO in handling complex structural optimization challenges.

Table 4: Comparison of optimal results of the 120-bar dome-like truss obtained by different algorithms

Element group A_i (cm^2)	IGSA [1]	OMGSA [1]	ISOS [50]	DPSO [47]	PSRO [51]	EBBO [52]	Jaya [53]	MS-TLBO [54]	PGO
1	19.043	20.263	19.6662	19.607	19.972	19.8878	19.309	19.4486	19.5059
2	41.418	39.294	39.8539	41.290	39.701	39.8248	40.763	40.3949	40.2263
3	10.218	9.989	10.6127	11.136	11.323	10.5496	10.791	10.6921	10.6113
4	20.664	20.563	21.2901	21.025	21.808	21.0929	21.272	21.3139	21.1780
5	10.795	9.603	9.7911	10.060	10.179	9.4245	9.943	9.8943	9.9194
6	12.190	11.738	11.7899	12.758	12.739	11.6648	11.695	11.7810	11.7999
7	14.960	15.877	14.7437	15.414	14.731	15.1282	14.579	14.5979	14.7623
Best weight (kg)	8727.28	8724.97	8710.0620	8890.48	8892.33	8711.95	8709.35	8708.729	8707.34
Average weight (kg)	8798.55	8745.58	8728.5951	8895.99	8921.3	8718.5	8713.21	8734.7450	8709.32
Worst weight (kg)	8800.45	8760.75	8770.8110	-	-	-	-	-	8718.55
Standard deviation (kg)	7.195	1.183	14.2296	4.26	18.54	7.15	2.97	27.0503	2.57
Number of FE analyses	4000	4000	4000	6000	4000	6500	18000	4000	18,780

[DOI: 10.22068/ijoce.2025.15.3.651]

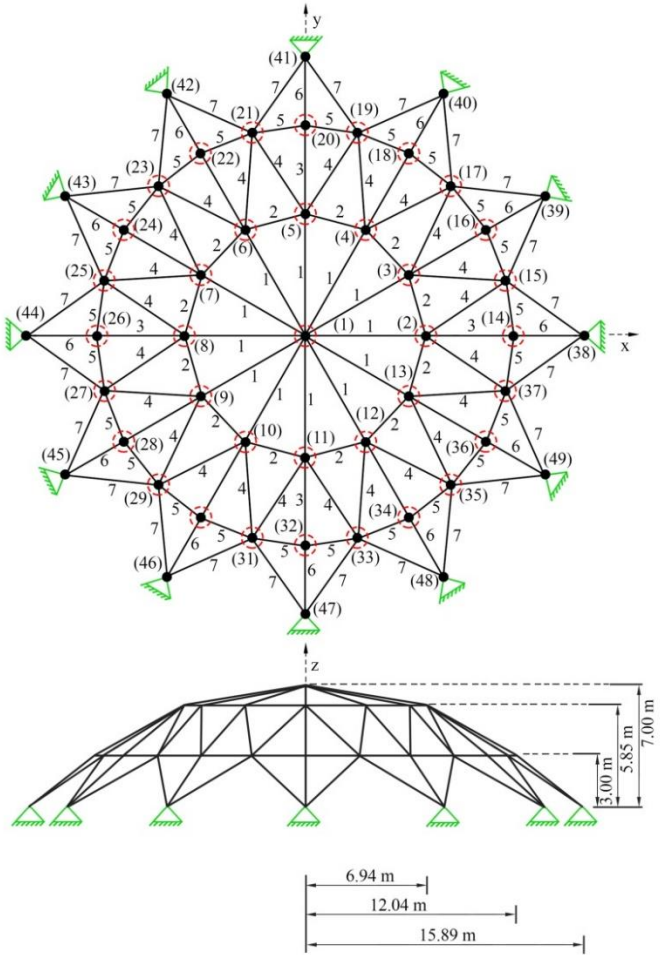

Figure 5: Schematic of the 120-bar dome-like truss

Table 5 Natural frequencies (Hz) of the optimal designs for the 120-bar dome-like truss

Frequency number	IGSA [1]	OMGSA [1]	ISOS [50]	DPSO [47]	PSRO [51]	EBBO [52]	Jaya [53]	MS-TLBO [54]	PGO
1	9.001	9.002	9.0001	9.0001	9.000	9.0000	9.0000	9.0002	9.0000
2	11.003	11.003	10.9998	11.0007	11.000	11.0000	11.0002	11.0000	11.0000
3	11.003	11.003	-	11.0053	11.005	11.0002	11.0002	11.0000	11.0000
4	11.017	11.007	-	11.0129	11.012	11.0008	11.0008	11.0006	11.0000
5	11.089	11.076	-	11.0471	11.045	11.0657	11.0674	11.0672	11.0671

4.3 A 600-bar dome-like truss

Figures 7 and 8 show the schematic of a 600-bar single-layer dome structure, which is considered as the last example. The entire structure is composed of 216 nodes and 600 elements. The structure has a cyclically repeated pattern and could be generated by the cyclic repetition of a sub-structure composed of 9 nodes and 25 elements. Symmetric dome-like truss

[DOI: 10.22068/ijoce.2025.15.3.651]

structures and other symmetric structures have been the subject of several group theoretic investigations mainly performed by Zingoni [55]. The angle of rotation of the sub-structure about the axis of revolution is 15°. The sub-structure is shown in Figure 9 in more detail for nodal numbering and coordinates. Table 6 lists the nodal coordinates of the typical sub-structure in the Cartesian coordinate system. Each element of the sub-structure is considered as a design variable. The layout of the structure is kept unchanged during the optimization process. Thus, this is a size optimization problem with 25 design variables. Material density, elasticity modulus, cross-sectional area bounds, and frequency constraints of the structure are listed in Table 1. A non-structural mass of 100 kg is attached to all free nodes of the dome. This problem has been investigated by several researchers via different optimization methods: Kaveh and Zolghadr [56] using DPSO, Kaveh and Ilchi Ghazaan [57] utilizing Vibrating Particles System (VPS), Kaveh and Ilchi Ghazaan [10] employing Enhanced Colliding Bodies Optimization (ECBO) and its cascade version, Kaveh and Ilchi Ghazaan [58] using VPS and its hybrid version, and Kaveh and Ilchi Ghazaan [59] utilizing Colliding Bodies Optimization (CBO), Kaveh et al. [60] using Improved Slime Mould (ISMA), Kaveh et al.[61] using Set-Theoretical-Based Jaya Algorithm (ST-JA), Kaveh et al. [62] using Success-History Based Adaptive Differential Evolution (SHADE) algorithm, and Kaveh et al. [63] using Improved Hybrid Growth Optimizer (IHGO).

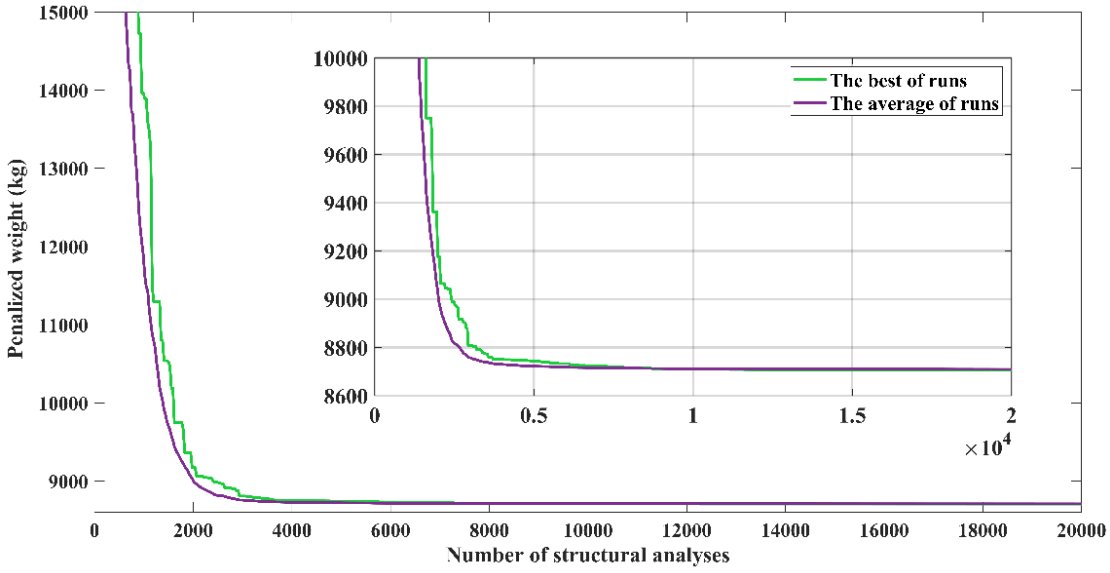

Figure 6: The best and average weight convergence histories for the 120-bar dome-like truss

A comparison of the optimal designs for the highly complex 600-bar dome-like truss, as summarized in Table 7, demonstrates the notable performance of the PGO algorithm. The results reveal that PGO achieves the lightest best-weight structure among all compared methods, with a recorded weight of 6066.74 kg. This represents a significant improvement over the best designs found by other advanced algorithms.

However, a more detailed examination of the statistical results reveals a distinct

[DOI: 10.22068/ijoce.2025.15.3.651]

characteristic of the PGO method. While it successfully located the lightest individual design, the algorithm's performance across multiple runs, as indicated by the higher average weight, worst weight, and substantial standard deviation of 557.22 kg, shows greater variability compared to several other methods. This suggests that while PGO is highly effective at exploring the design space to find a very low-weight solution, the consistency of its outcomes can vary. In terms of computational cost, PGO required 29,730 finite element analyses to converge, which is a moderate demand relative to the other algorithms applied to this large-scale problem.

The convergence history of PGO, illustrated in Figure 10, provides further insight. The plot shows a significant and rapid initial decrease in the best-found weight, underscoring the algorithm's strong exploratory capability in the early stages. The natural frequencies for the PGO-optimized design, presented in Table 8, confirm that all constraints are satisfactorily met, with the first two frequencies actively governing the design at their specified lower limits.

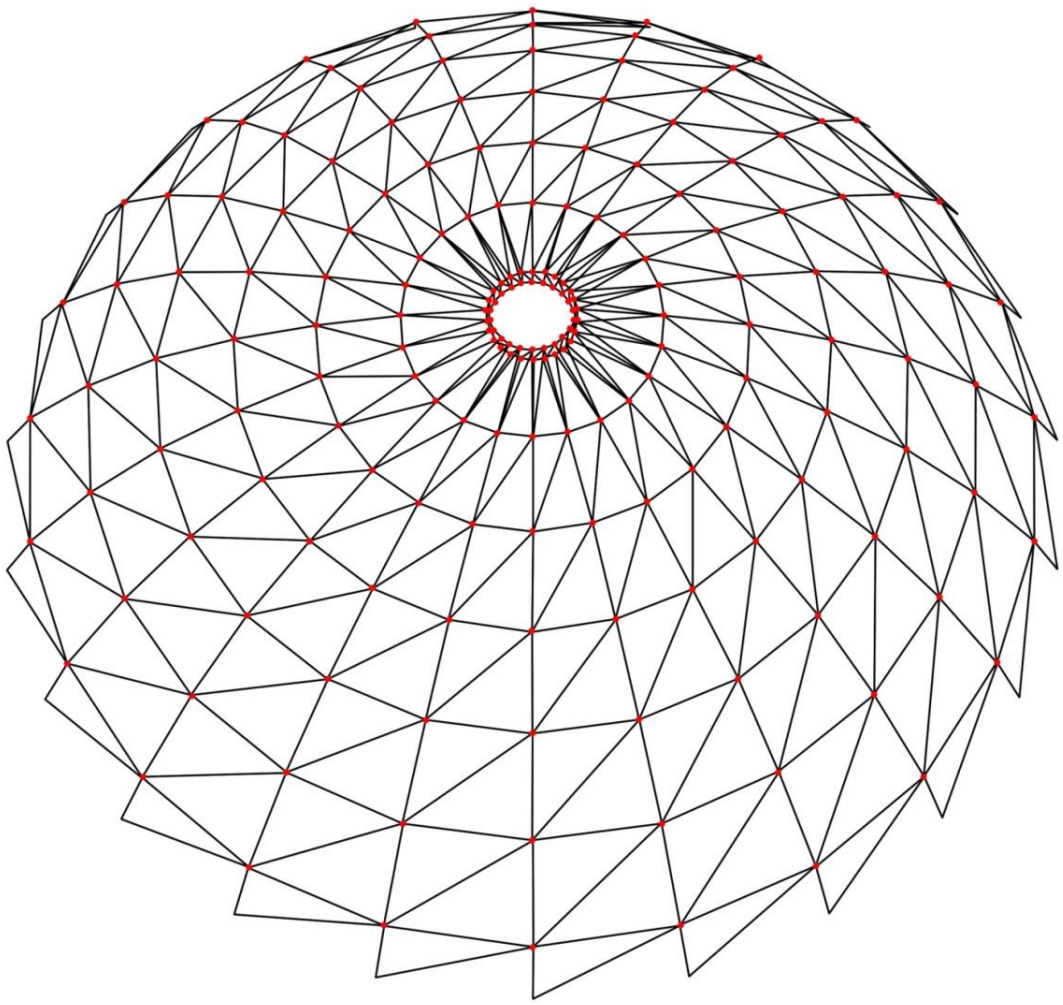

Figure 7: Schematic of the 600-bar single-layer dome

[DOI: 10.22068/ijoce.2025.15.3.651]

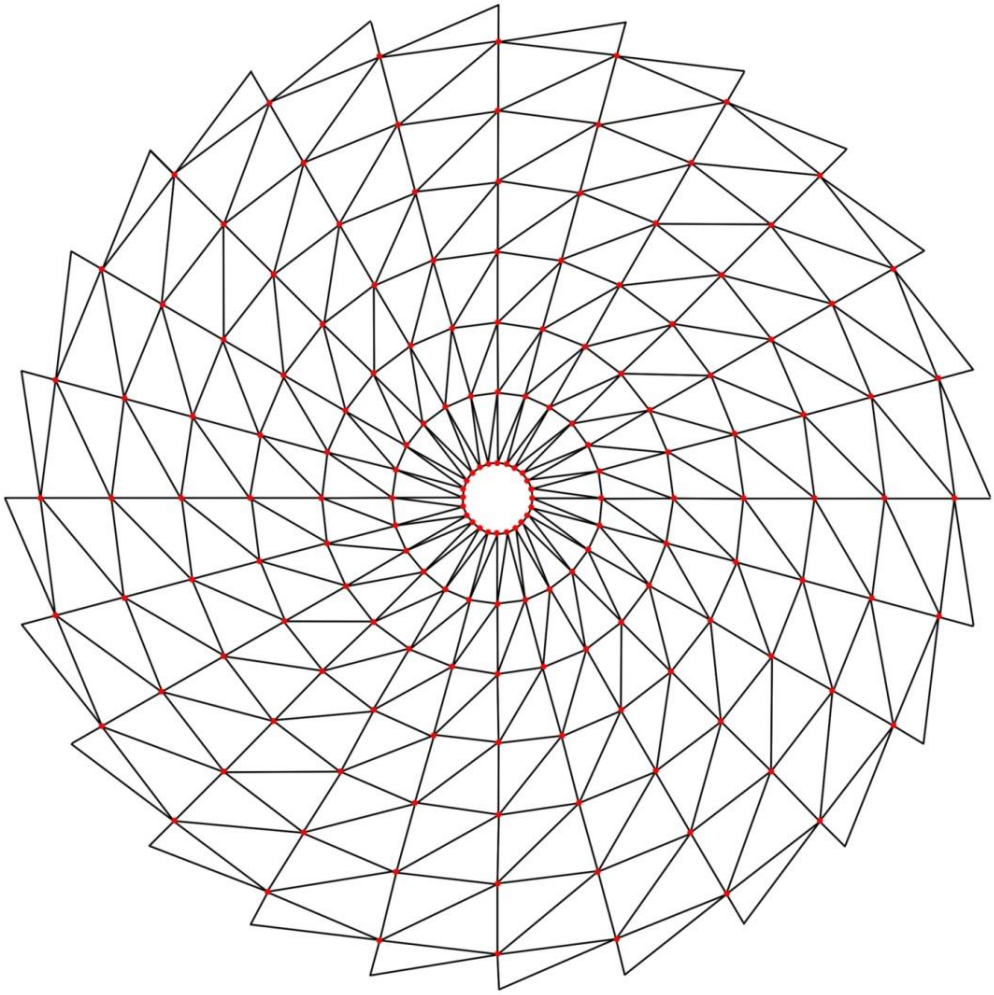

Figure 8: The 600-bar single-layer dome-like truss (top view)

Table 6: Coordinates of the nodes of the 600-bar dome-like truss

Node number	Coordinates (x, y, z) (m)
1	(1.0, 0.0, 7.0)
2	(1.0, 0.0, 7.5)
3	(3.0, 0.0, 7.25)
4	(5.0, 0.0, 6.75)
5	(7.0, 0.0, 6.0)
6	(9.0, 0.0, 5.0)
7	(11.0, 0.0, 3.5)
8	(13.0, 0.0, 1.5)
9	(14.0, 0.0, 0.0)

[DOI: 10.22068/ijoce.2025.15.3.651]

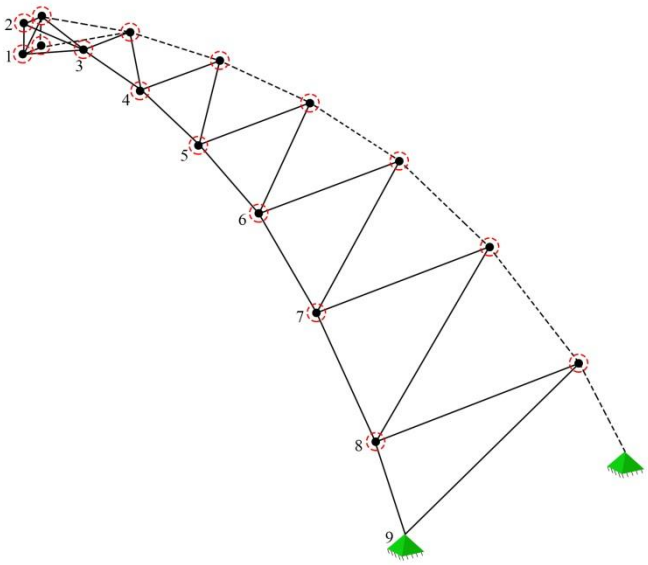

Figure 9: Details of a sub-structure of the 600-bar single-layer dome

Table 7: Comparison of optimal results of the 600-bar dome-like truss obtained by different algorithms

Element number (element nodes)	DPSO [56]	VPS [57]	ECBO [10]	ECBO-Cascade [10]	CBO [59]	VPS [58]	MDVC-UPVS [58]	PGO
1 (1-2)	1.365	1.3030	1.4305	1.0299	1.2404	1.3155	1.2575	1.2367
2 (1-3)	1.391	1.3998	1.3941	1.3664	1.3797	1.2299	1.3466	17.2123
3 (1-10)	5.686	5.1072	5.5293	5.1095	5.2597	5.5506	4.9738	12.9468
4 (1-11)	1.511	1.3882	1.0469	1.3011	1.2658	1.3867	1.4025	9.7043
5 (2-3)	17.711	16.9217	16.9642	17.0572	17.2255	17.4275	17.3802	6.8448
6 (2-11)	36.266	38.1432	35.1892	34.0764	38.2991	40.1430	37.9742	5.5899
7 (3-4)	13.263	11.8319	12.2171	13.0985	12.2234	12.8848	13.0306	4.2002
8 (3-11)	16.919	16.6149	16.7152	15.5882	15.4712	15.5413	15.9209	3.4860
9 (3-12)	13.333	11.3403	12.5999	12.6889	11.1577	12.2428	11.9419	1.3342
10 (4-5)	9.534	9.3865	9.5118	10.3314	9.4636	9.3776	9.1643	5.4125
11 (4-12)	9.884	8.7692	8.9977	8.5313	8.8250	8.6684	8.4332	37.9885
12 (4-13)	9.547	9.6682	9.4397	9.8308	9.1021	9.1659	9.2375	10.7810
13 (5-6)	7.866	6.9826	6.8864	7.0101	6.8417	7.1664	7.2213	8.9159
14 (5-13)	5.529	5.4445	4.2057	5.2917	5.2882	5.2170	5.2142	6.9115
15 (5-14)	7.007	6.3247	7.2651	6.2750	6.7702	6.5346	6.7961	7.6988
16 (6-7)	5.462	5.1349	6.1693	5.4305	5.1402	5.4741	5.2078	4.6182
17 (6-14)	3.853	3.3991	3.9768	3.6414	5.1827	3.6545	3.4586	4.5085
18 (6-15)	7.432	7.7911	8.3127	7.2827	7.4781	7.6034	7.6407	15.2861
19 (7-8)	4.261	4.4147	4.1451	4.4912	4.5646	4.2251	4.3690	8.3854
20 (7-15)	2.253	2.2755	2.4042	1.9275	1.8617	1.9717	2.1237	5.0823
21 (7-16)	4.337	4.9974	4.3038	4.6958	4.8797	4.5107	4.5774	3.6628
22 (8-9)	4.028	4.0145	3.2539	3.3595	3.5065	3.5251	3.4564	2.1247
23 (8-16)	1.954	1.8388	1.8273	1.7067	2.4546	1.9255	1.7920	1.8824
24 (8-17)	4.709	4.7965	4.8805	4.8372	4.9128	4.7628	4.8264	1.6597

[DOI: 10.22068/ijoce.2025.15.3.651]

25 (9-17)	1.410	1.5551	1.5276	2.0253	1.2324	1.6854	1.7601	1.6170
Best weight (kg)	6344.55	6133.02	6171.51	6140.51	6182.01	6120.01	6115.10	6066.74
Average weight (kg)	6674.71	6142.03	6191.50	6175.33	6226.37	6158.11	6119.95	6299.60
Worst weight (kg)	-	-	-	-	-	-	-	8136.73
Standard deviation (kg)	473.21	12.54	39.08	34.08	60.12	28.49	16.23	557.2235
Number of FE analyses	9000	30000	20000	20000	20000	30000	18000	29,730

Table 8: Natural frequencies (Hz) of the optimal designs for the 600-bar dome-like truss

Frequency number	DPSO [56]	VPS [57]	ECBO [10]	ECBO-Cascade [10]	CBO [59]	VPS [58]	MDVC-UPVS [58]	PGO
1	5.000	5.0000	5.002	5.001	5.000	5.000	5.000	5.0015
2	5.000	5.0003	5.003	5.001	5.000	5.000	5.000	5.0015
3	7.000	7.0000	7.001	7.001	7.000	7.000	7.000	7.0000
4	7.000	7.0001	7.001	7.001	7.000	7.000	7.000	7.0000
5	7.000	7.0002	7.002	7.002	7.001	7.000	7.000	7.0001

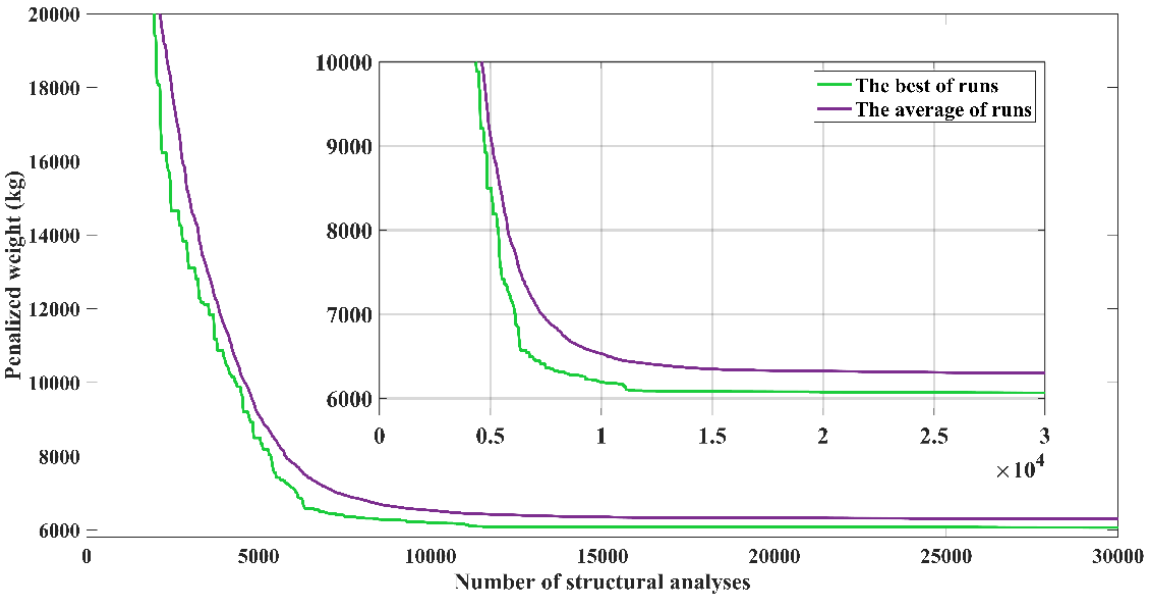

Figure 10: The best and average weight convergence histories for the 600-bar dome-like truss

[DOI: 10.22068/ijoce.2025.15.3.651]

5. CONCLUSIONS

The Plasma Generation Optimization (PGO) algorithm is a physically-based metaheuristic, recently developed and inspired by the energy transfer processes in plasma generation. In this paper, the standard PGO algorithm was successfully applied for the first time to the challenging domain of structural optimization with multiple frequency constraints. The algorithm's performance was rigorously evaluated on three dome truss benchmarks of increasing complexity: the 52-bar, 120-bar, and 600-bar structures.

Numerical results demonstrate that PGO is a highly competitive and effective optimizer for this class of problems. For the 52-bar and 120-bar domes, PGO achieved the lightest best-weight designs while maintaining strong statistical performance in terms of average and worst weights. In the case of the large-scale 600-bar dome, PGO identified the overall lightest design among all compared algorithms, showcasing its powerful global exploration capability, particularly through the Lévy-flight-driven ionization process. The inherent search mechanism of PGO, which balances global exploration (via ionization) with local refinement (via excitation and de-excitation), provides a robust foundation for navigating the highly non-linear and non-convex search spaces typical of frequency-constrained optimization. The convergence histories further confirm the algorithm's efficiency in steadily progressing towards high-quality, feasible designs.

The findings of this study confirm that the PGO algorithm can serve as a reliable and high-performance tool for solving complex truss optimization problems with dynamic constraints. Finally, the demonstrated potential of PGO suggests its promising applicability to a broader range of structural optimization challenges, such as frames, plates, and other engineering systems.

[DOI: 10.22068/ijoce.2025.15.3.651]

ACKNOWLEDGMENTS

This work is based upon research funded by Iran National Science Foundation (INSF) under project No. 4024911. The authors declare that they have no other known competing financial interests or personal relationships that could have appeared to influence the work reported in this paper.

REFERENCES

1. Khatibinia M, Naseralavi SS. Truss optimization on shape and sizing with frequency constraints based on orthogonal multi-gravitational search algorithm. *J Sound Vib*. 2014;**333**(24):6349–69.
2. Grandhi RV, Venkayya VB. Structural optimization with frequency constraints. *AIAA J*. 1988;**26**(7):858–66.
3. Bellagamba L, Yang TY. Minimum-mass truss structures with constraints on fundamental natural frequency. *AIAA J*. 1981;**19**(11):1452–58.

4. Tong WH, Liu GR. An optimization procedure for truss structures with discrete design variables and dynamic constraints. *Comput Struct*. 2001;**79**(2):155–62.
5. Sedaghati R, Suleman A, Tabarrok B. Structural optimization with frequency constraints using the finite element force method. *AIAA J*. 2002;**40**(2):382–88.
6. Lingyun W, Mei Z, Guang M, Guanghua L. Truss optimization on shape and sizing with frequency constraints based on genetic algorithm. *Comput Mech*. 2005;**35**(5):361–68.
7. Gomes HM. Truss optimization with dynamic constraints using a particle swarm algorithm. *Expert Syst Appl*. 2011;**38**(1):957–68.
8. Kaveh A, Zolghadr A. Truss optimization with natural frequency constraints using a hybridized CSS-BBBC algorithm with trap recognition capability. *Comput Struct*. 2012;**102–103**:14–27.
9. Kaveh A, Zolghadr A. Optimal design of cyclically symmetric trusses with frequency constraints using cyclical parthenogenesis algorithm. *Adv Struct Eng*. 2018;**21**(5):739–55.
10. Kaveh A, Ilchi Ghazaan M. Optimal design of dome truss structures with dynamic frequency constraints. *Struct Multidiscip Optim*. 2016;**53**(3):605–21.
11. Ho-Huu V, Nguyen-Thoi T, Vo-Duy T, Nguyen-Trang T. An improved differential evolution based on roulette wheel selection for shape and size optimization of truss structures with frequency constraints. *Neural Comput Appl*. 2018;**29**(1):167–85.
12. Lieu QX, Do DTT, Lee J. An adaptive hybrid evolutionary firefly algorithm for shape and size optimization of truss structures with frequency constraints. *Comput Struct*. 2018;**195**:99–112.
13. Kaveh A, Biabani Hamedani K, Kamalinejad M. Set theoretical variants of the teaching–learning-based optimization algorithm for optimal design of truss structures with multiple frequency constraints. *Acta Mech*. 2020;**231**(9):3645–72.
14. Grandhi R. Structural optimization with frequency constraints – A review. *AIAA J*. 1993;**31**(12):2296–303.
15. Hosseini SM, Dehcheshmeh MM, Amiri GG. Experimental and numerical structural damage detection using a combined modal strain energy and flexibility method. *Struct Eng Mech*. 2023;**87**(6):555–74.
16. Kaveh A, Hosseini SM. Design optimization of cable-equipped barrel vault structures using improved shuffled based Jaya algorithm. *Adv Eng Softw*. 2023;**176**:103406.
17. Kaveh A, Hosseini SM. Discrete and continuous sizing optimization of large-scale truss structures using DE-MEDT algorithm. *Int J Optim Civ Eng*. 2022;**12**(3):335–64.
18. Kaveh A, Javadi SM, Moghanni RM. Optimal structural control of tall buildings using tuned mass dampers via chaotic optimization algorithm. *Struct*. 2020;**28**:2704–13.
19. Yang XS. *Nature-Inspired Metaheuristic Algorithms*. Luniver Press; 2010.
20. Holland JH. *Adaptation in Natural and Artificial Systems*. MIT Press; 1992.
21. Kirkpatrick S, Gelatt CD Jr, Vecchi MP. Optimization by simulated annealing. *Science*. 1983;**220**(4598):671–80.

[DOI: 10.22068/ijoce.2025.15.3.651]

22. Kennedy J, Eberhart R. Particle swarm optimization. In: *Proc ICNN'95 Int Conf Neural Netw*. 1995;**4**:1942–48.
23. Dorigo M, Maniezzo V, Colorni A. Ant system: optimization by a colony of cooperating agents. *IEEE Trans Syst Man Cybern B*. 1996;**26**(1):29–41.
24. Karaboga D. An idea based on honey bee swarm for numerical optimization. Technical Report TR06. Erciyes University; 2005.
25. Das S, Suganthan PN. Differential evolution: a survey of the state-of-the-art. *IEEE Trans Evol Comput*. 2010;**15**(1):4–31.
26. Yang XS, Deb S. Cuckoo search via Lévy flights. In: *World Congress on Nature & Biologically Inspired Computing (NaBIC)*. 2009:210–14.
27. Rao RV, Savsani VJ, Vakharia DP. Teaching–learning-based optimization: a novel method for constrained mechanical design optimization problems. *Comput Aided Des*. 2011;**43**(3):303–15.
28. Yang XS, Gandomi AH. Bat algorithm: a novel approach for global engineering optimization. *Eng Comput*. 2012;**29**(5):464–83.
29. Mirjalili S, Mirjalili SM, Lewis A. Grey wolf optimizer. *Adv Eng Softw*. 2014;**69**:46–61.
30. Kaveh A, Talatahari S. A novel heuristic optimization method: charged system search. *Acta Mech*. 2010;**213**(3):267–89.
31. Kaveh A, Khayatazad M. A new meta-heuristic method: ray optimization. *Comput Struct*. 2012;**112**:283–94.
32. Kaveh A, Farhoudi N. A new optimization method: dolphin echolocation. *Adv Eng Softw*. 2013;**59**:53–70.
33. Kaveh A, Mahdavi VR. Colliding bodies optimization: a novel meta-heuristic method. *Comput Struct*. 2014;**139**:18–27.
34. Kaveh A, Bakhshpoori T. Water evaporation optimization: a novel physically inspired optimization algorithm. *Comput Struct*. 2016;**167**:69–85.
35. Kaveh A, Dadras Eslamlou A. A novel meta-heuristic optimization algorithm: thermal exchange optimization. *Adv Eng Softw*. 2017;**110**:69–84.
36. Kaveh A, Hosseini SM, Zaerreza A. A physics-based metaheuristic algorithm based on Doppler effect phenomenon and mean Euclidian distance threshold. *Period Polytech Civ Eng*. 2022;**66**(3):820–42.
37. Kaveh A, Akbari H, Hosseini SM. Plasma generation optimization: a new physically-based metaheuristic algorithm for solving constrained optimization problems. *Eng Comput*. 2020;**38**(4):1554–606.
38. Kaveh A, Hosseini SM, Akbari H. Efficiency of plasma generation optimization for structural damage identification of skeletal structures. *Iran J Sci Technol Trans Civ Eng*. 2021;**45**(4):2069–90.

[DOI: 10.22068/ijoce.2025.15.3.651]

39. Kaveh A, Hosseini SM, Zaerreza A. Size, layout, and topology optimization of skeletal structures using plasma generation optimization. *Iran J Sci Technol Trans Civ Eng*. 2021;**45**(2):513–43.
40. Kaveh A, Akbari H, Hosseini SM. Plasma generation optimization for optimal design of reinforced concrete cantilever retaining wall structures. *Iran J Sci Technol Trans Civ Eng*. 2022;**46**(2):1177–200.
41. Kaveh A, Biabani Hamedani K, Kamalinejad M. An enhanced forensic-based investigation algorithm for optimal design of frequency-constrained dome structures. *Comput Struct*. 2021;**256**:106643.
42. Kaveh A. *Advances in Metaheuristic Algorithms for Optimal Design of Structures*. Springer; 2014.
43. Joines JA, Houck CR. On the use of non-stationary penalty functions to solve nonlinear constrained optimization problems with GAs. In: *Proc IEEE Conf Evol Comput*. 1994:579–84.
44. Chopra A. *Dynamics of Structures*. Pearson Education; 2012.
45. Miguel LFF. Shape and size optimization of truss structures considering dynamic constraints through modern metaheuristic algorithms. *Expert Syst Appl*. 2012;**39**(10):9458–67.
46. Kaveh A, Zolghadr A. Truss optimization with natural frequency constraints using a hybridized CSS-BBBC algorithm with trap recognition capability. *Comput Struct*. 2012;**102**:14–27.
47. Kaveh A, Zolghadr A. Democratic PSO for truss layout and size optimization with frequency constraints. *Comput Struct*. 2014;**130**:10–21.
48. Ho-Huu V, Nguyen-Thoi T, Vo-Duy T, Nguyen-Trang T. Optimal design of truss structures with frequency constraints using improved differential evolution algorithm based on an adaptive mutation scheme. *Autom Constr*. 2016;**68**:81–94.
49. Kaveh A, Ilchi Ghazaan M. Hybridized optimization algorithms for design of trusses with multiple natural frequency constraints. *Adv Eng Softw*. 2015;**79**:137–47.
50. Tejani GG, Savsani VJ, Buresu G, Patel VK. Truss optimization with natural frequency bounds using improved symbiotic organisms search. *Knowl Based Syst*. 2018;**143**:162–78.
51. Kaveh A, Zolghadr A. A new PSRO algorithm for frequency constraint truss shape and size optimization. *Struct Eng Mech*. 2014;**52**(3):445–68.
52. Taheri SHS, Jalili S. Enhanced biogeography-based optimization: a new method for size and shape optimization of truss structures with natural frequency constraints. *Lat Am J Solids Struct*. 2016;**13**:1406–30.
53. Dede T, Grzywiński M, Rao RV. Jaya: a new meta-heuristic algorithm for the optimization of braced dome structures. In: *Adv Eng Optim Through Intell Tech*. Springer; 2019:13–20.

[DOI: 10.22068/ijoce.2025.15.3.651]

54. Tejani GG, Savsani VJ, Patel VK. Modified sub-population teaching-learning-based optimization for design of truss structures with natural frequency constraints. *Mech Based Des Struct Mach*. 2016;**44**(4):495–13.
55. Zingoni A. Symmetry recognition in group-theoretic computational schemes for complex structural systems. *Comput Struct*. 2012;**94**:34–44.
56. Kaveh A. Optimal analysis and design of large-scale domes with frequency constraints. In: *Applications of Metaheuristic Optimization Algorithms in Civil Engineering*. Springer; 2016:257–79.
57. Kaveh A, Ilchi Ghazaan M. Vibrating particles system algorithm for truss optimization with multiple natural frequency constraints. *Acta Mech*. 2017;**228**(1):307–22.
58. Kaveh A, Ilchi Ghazaan M. A new hybrid meta-heuristic algorithm for optimal design of large-scale dome structures. *Eng Optim*. 2018;**50**(2):235–52.
59. Kaveh A, Ghazaan MI. *Meta-Heuristic Algorithms for Optimal Design of Real-Size Structures*. Springer; 2018.
60. Kaveh A, Biabani Hamedani K, Kamalinejad M. Improved slime mould algorithm with elitist strategy and its application to structural optimization with natural frequency constraints. *Comput Struct*. 2022;**264**:106760.
61. Kaveh A, Biabani Hamedani K, Bakhshpoori T, Hamedani BB. Optimal analysis for optimal design of cyclic symmetric structures subject to frequency constraints. *Structures*. 2021;**33**:2522–41.
62. Kaveh A, Biabani Hamedani K, Hamedani BB. Optimal design of large-scale dome truss structures with multiple frequency constraints using success-history based adaptive differential evolution algorithm. *Period Polytech Civ Eng*. 2023;**67**(1):36–56.
63. Kaveh A, Biabani Hamedani K, Hosseini SM. Frequency-constrained optimization of large-scale cyclically symmetric domes using improved hybrid growth optimizer. *Scientia Iranica*. 2025.

[DOI: 10.22068/ijoce.2025.15.3.651]